August 2007

hep-ex/0708.1544

BABAR-PUB-07/047
SLAC-PUB-12727

Measurement of $\cos 2\beta$ in $B^0 \to D^{(*)}h^0$ Decays with a Time-Dependent Dalitz Plot Analysis of $D \to K^0_s\pi^+\pi^-$

B. Aubert,[1] M. Bona,[1] D. Boutigny,[1] Y. Karyotakis,[1] J. P. Lees,[1] V. Poireau,[1] X. Prudent,[1] V. Tisserand,[1] A. Zghiche,[1] J. Garra Tico,[2] E. Grauges,[2] L. Lopez,[3] A. Palano,[3] M. Pappagallo,[3] G. Eigen,[4] B. Stugu,[4] L. Sun,[4] G. S. Abrams,[5] M. Battaglia,[5] D. N. Brown,[5] J. Button-Shafer,[5] R. N. Cahn,[5] Y. Groysman,[5] R. G. Jacobsen,[5] J. A. Kadyk,[5] L. T. Kerth,[5] Yu. G. Kolomensky,[5] G. Kukartsev,[5] D. Lopes Pegna,[5] G. Lynch,[5] L. M. Mir,[5] T. J. Orimoto,[5] I. L. Osipenkov,[5] M. T. Ronan,[5,*] K. Tackmann,[5] T. Tanabe,[5] W. A. Wenzel,[5] P. del Amo Sanchez,[6] C. M. Hawkes,[6] A. T. Watson,[6] H. Koch,[7] T. Schroeder,[7] D. Walker,[8] D. J. Asgeirsson,[9] T. Cuhadar-Donszelmann,[9] B. G. Fulsom,[9] C. Hearty,[9] T. S. Mattison,[9] J. A. McKenna,[9] A. Khan,[10] M. Saleem,[10] L. Teodorescu,[10] V. E. Blinov,[11] A. D. Bukin,[11] V. P. Druzhinin,[11] V. B. Golubev,[11] A. P. Onuchin,[11] S. I. Serednyakov,[11] Yu. I. Skovpen,[11] E. P. Solodov,[11] K. Yu. Todyshev,[11] M. Bondioli,[12] S. Curry,[12] I. Eschrich,[12] D. Kirkby,[12] A. J. Lankford,[12] P. Lund,[12] M. Mandelkern,[12] E. C. Martin,[12] D. P. Stoker,[12] S. Abachi,[13] C. Buchanan,[13] S. D. Foulkes,[14] J. W. Gary,[14] F. Liu,[14] O. Long,[14] B. C. Shen,[14] G. M. Vitug,[14] L. Zhang,[14] H. P. Paar,[15] S. Rahatlou,[15] V. Sharma,[15] J. W. Berryhill,[16] C. Campagnari,[16] A. Cunha,[16] B. Dahmes,[16] T. M. Hong,[16] D. Kovalskyi,[16] J. D. Richman,[16] T. W. Beck,[17] A. M. Eisner,[17] C. J. Flacco,[17] C. A. Heusch,[17] J. Kroseberg,[17] W. S. Lockman,[17] T. Schalk,[17] B. A. Schumm,[17] A. Seiden,[17] M. G. Wilson,[17] L. O. Winstrom,[17] E. Chen,[18] C. H. Cheng,[18] F. Fang,[18] D. G. Hitlin,[18] I. Narsky,[18] T. Piatenko,[18] F. C. Porter,[18] R. Andreassen,[19] G. Mancinelli,[19] B. T. Meadows,[19] K. Mishra,[19] M. D. Sokoloff,[19] F. Blanc,[20] P. C. Bloom,[20] S. Chen,[20] W. T. Ford,[20] J. F. Hirschauer,[20] A. Kreisel,[20] M. Nagel,[20] U. Nauenberg,[20] A. Olivas,[20] J. G. Smith,[20] K. A. Ulmer,[20] S. R. Wagner,[20] J. Zhang,[20] A. M. Gabareen,[21] A. Soffer,[21,†] W. H. Toki,[21] R. J. Wilson,[21] F. Winklmeier,[21] D. D. Altenburg,[22] E. Feltresi,[22] A. Hauke,[22] H. Jasper,[22] J. Merkel,[22] A. Petzold,[22] B. Spaan,[22] K. Wacker,[22] V. Klose,[23] M. J. Kobel,[23] H. M. Lacker,[23] W. F. Mader,[23] R. Nogowski,[23] J. Schubert,[23] K. R. Schubert,[23] R. Schwierz,[23] J. E. Sundermann,[23] A. Volk,[23] D. Bernard,[24] G. R. Bonneaud,[24] E. Latour,[24] V. Lombardo,[24] Ch. Thiebaux,[24] M. Verderi,[24] P. J. Clark,[25] W. Gradl,[25] F. Muheim,[25] S. Playfer,[25] A. I. Robertson,[25] J. E. Watson,[25] Y. Xie,[25] M. Andreotti,[26] D. Bettoni,[26] C. Bozzi,[26] R. Calabrese,[26] A. Cecchi,[26] G. Cibinetto,[26] P. Franchini,[26] E. Luppi,[26] M. Negrini,[26] A. Petrella,[26] L. Piemontese,[26] E. Prencipe,[26] V. Santoro,[26] F. Anulli,[27] R. Baldini-Ferroli,[27] A. Calcaterra,[27] R. de Sangro,[27] G. Finocchiaro,[27] S. Pacetti,[27] P. Patteri,[27] I. M. Peruzzi,[27,‡] M. Piccolo,[27] M. Rama,[27] A. Zallo,[27] A. Buzzo,[28] R. Contri,[28] M. Lo Vetere,[28] M. M. Macri,[28] M. R. Monge,[28] S. Passaggio,[28] C. Patrignani,[28] E. Robutti,[28] A. Santroni,[28] S. Tosi,[28] K. S. Chaisanguanthum,[29] M. Morii,[29] J. Wu,[29] R. S. Dubitzky,[30] J. Marks,[30] S. Schenk,[30] U. Uwer,[30] D. J. Bard,[31] P. D. Dauncey,[31] R. L. Flack,[31] J. A. Nash,[31] W. Panduro Vazquez,[31] M. Tibbetts,[31] P. K. Behera,[32] X. Chai,[32] M. J. Charles,[32] U. Mallik,[32] J. Cochran,[33] H. B. Crawley,[33] L. Dong,[33] V. Eyges,[33] W. T. Meyer,[33] S. Prell,[33] E. I. Rosenberg,[33] A. E. Rubin,[33] Y. Y. Gao,[34] A. V. Gritsan,[34] Z. J. Guo,[34] C. K. Lae,[34] A. G. Denig,[35] M. Fritsch,[35] G. Schott,[35] N. Arnaud,[36] J. Béquilleux,[36] A. D'Orazio,[36] M. Davier,[36] G. Grosdidier,[36] A. Höcker,[36] V. Lepeltier,[36] F. Le Diberder,[36] A. M. Lutz,[36] S. Pruvot,[36] S. Rodier,[36] P. Roudeau,[36] M. H. Schune,[36] J. Serrano,[36] V. Sordini,[36] A. Stocchi,[36] W. F. Wang,[36] G. Wormser,[36] D. J. Lange,[37] D. M. Wright,[37] I. Bingham,[38] C. A. Chavez,[38] J. R. Fry,[38] E. Gabathuler,[38] R. Gamet,[38] D. E. Hutchcroft,[38] D. J. Payne,[38] K. C. Schofield,[38] C. Touramanis,[38] A. J. Bevan,[39] K. A. George,[39] F. Di Lodovico,[39] R. Sacco,[39] G. Cowan,[40] H. U. Flaecher,[40] D. A. Hopkins,[40] S. Paramesvaran,[40] F. Salvatore,[40] A. C. Wren,[40] D. N. Brown,[41] C. L. Davis,[41] J. Allison,[42] D. Bailey,[42] N. R. Barlow,[42] R. J. Barlow,[42] Y. M. Chia,[42] C. L. Edgar,[42] G. D. Lafferty,[42] T. J. West,[42] J. I. Yi,[42] J. Anderson,[43] C. Chen,[43] A. Jawahery,[43] D. A. Roberts,[43] G. Simi,[43] J. M. Tuggle,[43] G. Blaylock,[44] C. Dallapiccola,[44] S. S. Hertzbach,[44] X. Li,[44] T. B. Moore,[44] E. Salvati,[44] S. Saremi,[44] R. Cowan,[45] D. Dujmic,[45] P. H. Fisher,[45] K. Koeneke,[45] G. Sciolla,[45] M. Spitznagel,[45] F. Taylor,[45] R. K. Yamamoto,[45] M. Zhao,[45] Y. Zheng,[45] S. E. Mclachlin,[46,*] P. M. Patel,[46] S. H. Robertson,[46] A. Lazzaro,[47] F. Palombo,[47] J. M. Bauer,[48] L. Cremaldi,[48] V. Eschenburg,[48] R. Godang,[48] R. Kroeger,[48] D. A. Sanders,[48] D. J. Summers,[48] H. W. Zhao,[48] S. Brunet,[49] D. Côté,[49] M. Simard,[49] P. Taras,[49] F. B. Viaud,[49] H. Nicholson,[50] G. De Nardo,[51] F. Fabozzi,[51,§] L. Lista,[51] D. Monorchio,[51] C. Sciacca,[51] M. A. Baak,[52] G. Raven,[52] H. L. Snoek,[52] C. P. Jessop,[53] K. J. Knoepfel,[53] J. M. LoSecco,[53] G. Benelli,[54] L. A. Corwin,[54] K. Honscheid,[54] H. Kagan,[54] R. Kass,[54]

Submitted to Physical Review Letters

Work supported in part by US Department of Energy contract DE-AC02-76SF00515

J. P. Morris,[54] A. M. Rahimi,[54] J. J. Regensburger,[54] S. J. Sekula,[54] Q. K. Wong,[54] N. L. Blount,[55] J. Brau,[55] R. Frey,[55] O. Igonkina,[55] J. A. Kolb,[55] M. Lu,[55] R. Rahmat,[55] N. B. Sinev,[55] D. Strom,[55] J. Strube,[55] E. Torrence,[55] N. Gagliardi,[56] A. Gaz,[56] M. Margoni,[56] M. Morandin,[56] A. Pompili,[56] M. Posocco,[56] M. Rotondo,[56] F. Simonetto,[56] R. Stroili,[56] C. Voci,[56] E. Ben-Haim,[57] H. Briand,[57] G. Calderini,[57] J. Chauveau,[57] P. David,[57] L. Del Buono,[57] Ch. de la Vaissière,[57] O. Hamon,[57] Ph. Leruste,[57] J. Malclès,[57] J. Ocariz,[57] A. Perez,[57] J. Prendki,[57] L. Gladney,[58] M. Biasini,[59] R. Covarelli,[59] E. Manoni,[59] C. Angelini,[60] G. Batignani,[60] S. Bettarini,[60] M. Carpinelli,[60] R. Cenci,[60] A. Cervelli,[60] F. Forti,[60] M. A. Giorgi,[60] A. Lusiani,[60] G. Marchiori,[60] M. A. Mazur,[60] M. Morganti,[60] N. Neri,[60] E. Paoloni,[60] G. Rizzo,[60] J. J. Walsh,[60] J. Biesiada,[61] P. Elmer,[61] Y. P. Lau,[61] C. Lu,[61] J. Olsen,[61] A. J. S. Smith,[61] A. V. Telnov,[61] E. Baracchini,[62] F. Bellini,[62] G. Cavoto,[62] D. del Re,[62] E. Di Marco,[62] R. Faccini,[62] F. Ferrarotto,[62] F. Ferroni,[62] M. Gaspero,[62] P. D. Jackson,[62] L. Li Gioi,[62] M. A. Mazzoni,[62] S. Morganti,[62] G. Piredda,[62] F. Polci,[62] F. Renga,[62] C. Voena,[62] M. Ebert,[63] T. Hartmann,[63] H. Schröder,[63] R. Waldi,[63] T. Adye,[64] G. Castelli,[64] B. Franek,[64] E. O. Olaiya,[64] W. Roethel,[64] F. F. Wilson,[64] S. Emery,[65] M. Escalier,[65] A. Gaidot,[65] S. F. Ganzhur,[65] G. Hamel de Monchenault,[65] W. Kozanecki,[65] G. Vasseur,[65] Ch. Yèche,[65] M. Zito,[65] X. R. Chen,[66] H. Liu,[66] W. Park,[66] M. V. Purohit,[66] R. M. White,[66] J. R. Wilson,[66] M. T. Allen,[67] D. Aston,[67] R. Bartoldus,[67] P. Bechtle,[67] R. Claus,[67] J. P. Coleman,[67] M. R. Convery,[67] J. C. Dingfelder,[67] J. Dorfan,[67] G. P. Dubois-Felsmann,[67] W. Dunwoodie,[67] R. C. Field,[67] T. Glanzman,[67] S. J. Gowdy,[67] M. T. Graham,[67] P. Grenier,[67] C. Hast,[67] W. R. Innes,[67] J. Kaminski,[67] M. H. Kelsey,[67] H. Kim,[67] P. Kim,[67] M. L. Kocian,[67] D. W. G. S. Leith,[67] S. Li,[67] S. Luitz,[67] V. Luth,[67] H. L. Lynch,[67] D. B. MacFarlane,[67] H. Marsiske,[67] R. Messner,[67] D. R. Muller,[67] C. P. O'Grady,[67] I. Ofte,[67] A. Perazzo,[67] M. Perl,[67] T. Pulliam,[67] B. N. Ratcliff,[67] A. Roodman,[67] A. A. Salnikov,[67] R. H. Schindler,[67] J. Schwiening,[67] A. Snyder,[67] D. Su,[67] M. K. Sullivan,[67] K. Suzuki,[67] S. K. Swain,[67] J. M. Thompson,[67] J. Va'vra,[67] A. P. Wagner,[67] M. Weaver,[67] W. J. Wisniewski,[67] M. Wittgen,[67] D. H. Wright,[67] A. K. Yarritu,[67] K. Yi,[67] C. C. Young,[67] V. Ziegler,[67] P. R. Burchat,[68] A. J. Edwards,[68] S. A. Majewski,[68] T. S. Miyashita,[68] B. A. Petersen,[68] L. Wilden,[68] S. Ahmed,[69] M. S. Alam,[69] R. Bula,[69] J. A. Ernst,[69] V. Jain,[69] B. Pan,[69] M. A. Saeed,[69] F. R. Wappler,[69] S. B. Zain,[69] M. Krishnamurthy,[70] S. M. Spanier,[70] R. Eckmann,[71] J. L. Ritchie,[71] A. M. Ruland,[71] C. J. Schilling,[71] R. F. Schwitters,[71] J. M. Izen,[72] X. C. Lou,[72] S. Ye,[72] F. Bianchi,[73] F. Gallo,[73] D. Gamba,[73] M. Pelliccioni,[73] M. Bomben,[74] L. Bosisio,[74] C. Cartaro,[74] F. Cossutti,[74] G. Della Ricca,[74] L. Lanceri,[74] L. Vitale,[74] V. Azzolini,[75] N. Lopez-March,[75] F. Martinez-Vidal,[75,¶] D. A. Milanes,[75] A. Oyanguren,[75] J. Albert,[76] Sw. Banerjee,[76] B. Bhuyan,[76] K. Hamano,[76] R. Kowalewski,[76] I. M. Nugent,[76] J. M. Roney,[76] R. J. Sobie,[76] P. F. Harrison,[77] J. Ilic,[77] T. E. Latham,[77] G. B. Mohanty,[77] H. R. Band,[78] X. Chen,[78] S. Dasu,[78] K. T. Flood,[78] J. J. Hollar,[78] P. E. Kutter,[78] Y. Pan,[78] M. Pierini,[78] R. Prepost,[78] S. L. Wu,[78] and H. Neal[79]

(The *BABAR* Collaboration)

[1]*Laboratoire de Physique des Particules, IN2P3/CNRS et Université de Savoie, F-74941 Annecy-Le-Vieux, France*
[2]*Universitat de Barcelona, Facultat de Fisica, Departament ECM, E-08028 Barcelona, Spain*
[3]*Università di Bari, Dipartimento di Fisica and INFN, I-70126 Bari, Italy*
[4]*University of Bergen, Institute of Physics, N-5007 Bergen, Norway*
[5]*Lawrence Berkeley National Laboratory and University of California, Berkeley, California 94720, USA*
[6]*University of Birmingham, Birmingham, B15 2TT, United Kingdom*
[7]*Ruhr Universität Bochum, Institut für Experimentalphysik 1, D-44780 Bochum, Germany*
[8]*University of Bristol, Bristol BS8 1TL, United Kingdom*
[9]*University of British Columbia, Vancouver, British Columbia, Canada V6T 1Z1*
[10]*Brunel University, Uxbridge, Middlesex UB8 3PH, United Kingdom*
[11]*Budker Institute of Nuclear Physics, Novosibirsk 630090, Russia*
[12]*University of California at Irvine, Irvine, California 92697, USA*
[13]*University of California at Los Angeles, Los Angeles, California 90024, USA*
[14]*University of California at Riverside, Riverside, California 92521, USA*
[15]*University of California at San Diego, La Jolla, California 92093, USA*
[16]*University of California at Santa Barbara, Santa Barbara, California 93106, USA*
[17]*University of California at Santa Cruz, Institute for Particle Physics, Santa Cruz, California 95064, USA*
[18]*California Institute of Technology, Pasadena, California 91125, USA*
[19]*University of Cincinnati, Cincinnati, Ohio 45221, USA*
[20]*University of Colorado, Boulder, Colorado 80309, USA*
[21]*Colorado State University, Fort Collins, Colorado 80523, USA*
[22]*Universität Dortmund, Institut für Physik, D-44221 Dortmund, Germany*
[23]*Technische Universität Dresden, Institut für Kern- und Teilchenphysik, D-01062 Dresden, Germany*
[24]*Laboratoire Leprince-Ringuet, CNRS/IN2P3, Ecole Polytechnique, F-91128 Palaiseau, France*

[25]University of Edinburgh, Edinburgh EH9 3JZ, United Kingdom
[26]Università di Ferrara, Dipartimento di Fisica and INFN, I-44100 Ferrara, Italy
[27]Laboratori Nazionali di Frascati dell'INFN, I-00044 Frascati, Italy
[28]Università di Genova, Dipartimento di Fisica and INFN, I-16146 Genova, Italy
[29]Harvard University, Cambridge, Massachusetts 02138, USA
[30]Universität Heidelberg, Physikalisches Institut, Philosophenweg 12, D-69120 Heidelberg, Germany
[31]Imperial College London, London, SW7 2AZ, United Kingdom
[32]University of Iowa, Iowa City, Iowa 52242, USA
[33]Iowa State University, Ames, Iowa 50011-3160, USA
[34]Johns Hopkins University, Baltimore, Maryland 21218, USA
[35]Universität Karlsruhe, Institut für Experimentelle Kernphysik, D-76021 Karlsruhe, Germany
[36]Laboratoire de l'Accélérateur Linéaire, IN2P3/CNRS et Université Paris-Sud 11,
Centre Scientifique d'Orsay, B. P. 34, F-91898 ORSAY Cedex, France
[37]Lawrence Livermore National Laboratory, Livermore, California 94550, USA
[38]University of Liverpool, Liverpool L69 7ZE, United Kingdom
[39]Queen Mary, University of London, E1 4NS, United Kingdom
[40]University of London, Royal Holloway and Bedford New College, Egham, Surrey TW20 0EX, United Kingdom
[41]University of Louisville, Louisville, Kentucky 40292, USA
[42]University of Manchester, Manchester M13 9PL, United Kingdom
[43]University of Maryland, College Park, Maryland 20742, USA
[44]University of Massachusetts, Amherst, Massachusetts 01003, USA
[45]Massachusetts Institute of Technology, Laboratory for Nuclear Science, Cambridge, Massachusetts 02139, USA
[46]McGill University, Montréal, Québec, Canada H3A 2T8
[47]Università di Milano, Dipartimento di Fisica and INFN, I-20133 Milano, Italy
[48]University of Mississippi, University, Mississippi 38677, USA
[49]Université de Montréal, Physique des Particules, Montréal, Québec, Canada H3C 3J7
[50]Mount Holyoke College, South Hadley, Massachusetts 01075, USA
[51]Università di Napoli Federico II, Dipartimento di Scienze Fisiche and INFN, I-80126, Napoli, Italy
[52]NIKHEF, National Institute for Nuclear Physics and High Energy Physics, NL-1009 DB Amsterdam, The Netherlands
[53]University of Notre Dame, Notre Dame, Indiana 46556, USA
[54]Ohio State University, Columbus, Ohio 43210, USA
[55]University of Oregon, Eugene, Oregon 97403, USA
[56]Università di Padova, Dipartimento di Fisica and INFN, I-35131 Padova, Italy
[57]Laboratoire de Physique Nucléaire et de Hautes Energies,
IN2P3/CNRS, Université Pierre et Marie Curie-Paris6,
Université Denis Diderot-Paris7, F-75252 Paris, France
[58]University of Pennsylvania, Philadelphia, Pennsylvania 19104, USA
[59]Università di Perugia, Dipartimento di Fisica and INFN, I-06100 Perugia, Italy
[60]Università di Pisa, Dipartimento di Fisica, Scuola Normale Superiore and INFN, I-56127 Pisa, Italy
[61]Princeton University, Princeton, New Jersey 08544, USA
[62]Università di Roma La Sapienza, Dipartimento di Fisica and INFN, I-00185 Roma, Italy
[63]Universität Rostock, D-18051 Rostock, Germany
[64]Rutherford Appleton Laboratory, Chilton, Didcot, Oxon, OX11 0QX, United Kingdom
[65]DSM/Dapnia, CEA/Saclay, F-91191 Gif-sur-Yvette, France
[66]University of South Carolina, Columbia, South Carolina 29208, USA
[67]Stanford Linear Accelerator Center, Stanford, California 94309, USA
[68]Stanford University, Stanford, California 94305-4060, USA
[69]State University of New York, Albany, New York 12222, USA
[70]University of Tennessee, Knoxville, Tennessee 37996, USA
[71]University of Texas at Austin, Austin, Texas 78712, USA
[72]University of Texas at Dallas, Richardson, Texas 75083, USA
[73]Università di Torino, Dipartimento di Fisica Sperimentale and INFN, I-10125 Torino, Italy
[74]Università di Trieste, Dipartimento di Fisica and INFN, I-34127 Trieste, Italy
[75]IFIC, Universitat de Valencia-CSIC, E-46071 Valencia, Spain
[76]University of Victoria, Victoria, British Columbia, Canada V8W 3P6
[77]Department of Physics, University of Warwick, Coventry CV4 7AL, United Kingdom
[78]University of Wisconsin, Madison, Wisconsin 53706, USA
[79]Yale University, New Haven, Connecticut 06511, USA

(Dated: August 11, 2007)

We study the time-dependent Dalitz plot of $D \to K^0_S\pi^+\pi^-$ in $B^0 \to D^{(*)}h^0$ decays, where h^0 is a π^0, η, η', or ω meson and $D^* \to D\pi^0$, using a data sample of 383×10^6 $\Upsilon(4S) \to B\overline{B}$ decays collected with the *BABAR* detector. We determine $\cos 2\beta = 0.42 \pm 0.49 \pm 0.09 \pm 0.13$, $\sin 2\beta = 0.29 \pm 0.34 \pm 0.03 \pm 0.05$, and $|\lambda| = 1.01 \pm 0.08 \pm 0.02$, where the first error is statistical, the second is

the experimental systematic uncertainty, and the third, where given, is the Dalitz model uncertainty. Assuming the world average value for $\sin 2\beta$ and $|\lambda| = 1$, $\cos 2\beta > 0$ is preferred over $\cos 2\beta < 0$ at 86% confidence level.

PACS numbers: 13.25.Hw, 12.15.Hh, 11.30.Er

Time-dependent *CP* asymmetries in B^0 meson decays, resulting from the interference between decays with and without B^0-$\overline{B}^0$ mixing, have been studied with high precision in $b \to c\overline{c}s$ decay modes by the *BABAR* and Belle collaborations [1]. These studies measure the asymmetry amplitude $\sin 2\beta$, where $\beta = -\arg(V_{cd}V_{cb}^*/V_{td}V_{tb}^*)$ is a phase in the Cabibbo-Kobayashi-Maskawa (CKM) quark-mixing matrix [2], $\boldsymbol{V}$. The *CP* violating phase 2β, inferred from $\sin 2\beta$, has a two-fold ambiguity, 2β and $\pi - 2\beta$ (four-fold ambiguity in β). This ambiguity can be resolved by studying decay modes that involve multibody final states $B^0 \to J/\psi K_S^0\pi^0$ [3], $D[K_S^0\pi^+\pi^-]h^0$ [4], $D^{*+}D^{*-}K_S^0$ [5] or $K^+K^-K^0$ [6], where the knowledge of the variation of the strong phase differences as a function of phase space allows one also to measure $\cos 2\beta$.

In this Letter, we present a study of *CP* asymmetry in $B^0 \to D^{(*)}h^0$ [7] decays with a time-dependent Dalitz plot analysis of $D \to K_S^0\pi^+\pi^-$ [8], where h^0 is a π^0, η, η', or ω meson. The $B^0 \to D^{(*)}h^0$ decay is dominated by a color-suppressed $\overline{b} \to \overline{c}u\overline{d}$ tree amplitude. The diagram $\overline{b} \to \overline{u}\overline{q}$, which involves a different weak phase, is suppressed by $V_{ub}V_{cd}^*/V_{cb}V_{ud}^* \simeq 0.02$. Neglecting the suppressed amplitude, we factorize the decay amplitude of the chain $B^0 \to \overline{D}^0h^0 \to [K_S^0\pi^+\pi^-]h^0$ into $\mathcal{A}_f = \mathcal{A}_B\mathcal{A}_{\overline{D}^0}$ and similarly for $\overline{B}^0$ into $\overline{\mathcal{A}}_{\overline{f}} = \mathcal{A}_{\overline{B}}\mathcal{A}_{D^0}$. The D^0 and $\overline{D}^0$ decay amplitudes are functions of the Dalitz plot variables $\mathcal{A}_{D^0} = f(m_+^2, m_-^2)$ and $\mathcal{A}_{\overline{D}^0} = \overline{f}(m_+^2, m_-^2) = f(m_-^2, m_+^2)$, where $m_\pm^2 \equiv m_{K_S^0\pi^\pm}^2$. In the $\Upsilon(4S) \to B^0\overline{B}^0$ system, the rate of a neutral B meson decaying at proper decay time $t_{\rm rec}$, the other B ($B_{\rm tag}$) at $t_{\rm tag}$, and the D decaying at a point on the Dalitz plot, is proportional to

$$\begin{aligned}\frac{e^{-\Gamma\Delta t}}{2}|\mathcal{A}_B|^2 \cdot \Big[&(|\mathcal{A}_{\overline{D}^0}|^2 + |\lambda|^2|\mathcal{A}_{D^0}|^2) \\ &\mp (|\mathcal{A}_{\overline{D}^0}|^2 - |\lambda|^2|\mathcal{A}_{D^0}|^2)\cos(\Delta m\Delta t) \\ &\pm 2|\lambda|\xi_{h^0}(-1)^L{\rm Im}(e^{-2i\beta}\mathcal{A}_{D^0}\mathcal{A}_{\overline{D}^0}^*)\sin(\Delta m\Delta t)\Big],\end{aligned} \quad (1)$$

where the upper (lower) sign is for events with $B_{\rm tag}$ decaying as a B^0 ($\overline{B}^0$), $\Delta t = t_{\rm rec} - t_{\rm tag}$, Γ is the decay rate of the neutral B meson, $\lambda = e^{-2i\beta}(\mathcal{A}_{\overline{B}}/\mathcal{A}_B)$, Δm is the B^0-$\overline{B}^0$ mixing frequency, ξ_{h^0} is the *CP* eigenvalue of h^0, and $(-1)^L$ is the orbital angular momentum factor. Here we have assumed *CP*-conservation in mixing and neglected decay width differences. For Dh^0 modes, $\xi_{h^0}(-1)^L = -1$. For $D^*[D\pi^0]h^0$ ($h^0 \neq \omega$) modes $\xi_{h^0}(-1)^L = +1$ including factors from D^* decay [9]. In the last term of expression 1 we can rewrite

$$\begin{aligned}{\rm Im}(e^{-2i\beta}\mathcal{A}_{D^0}\mathcal{A}_{\overline{D}^0}^*) = {\rm Im}(\mathcal{A}_{D^0}\mathcal{A}_{\overline{D}^0}^*)\cos 2\beta \\ - {\rm Re}(\mathcal{A}_{D^0}\mathcal{A}_{\overline{D}^0}^*)\sin 2\beta,\end{aligned} \quad (2)$$

and treat $\cos 2\beta$ and $\sin 2\beta$ as independent parameters.

We fully reconstruct $B^0 \to D^{(*)}h^0$ candidates from a data sample of $(383\pm4)\times10^6$ $\Upsilon(4S)$ decays into $B\overline{B}$ pairs collected with the *BABAR* detector at the asymmetric-energy e^+e^- PEP-II collider. The *BABAR* detector is described in detail elsewhere [10]. The decay modes used are $D\pi^0$, $D\eta$, $D\eta'$, $D\omega$, $D^*\pi^0$, and $D^*\eta$, with $D^* \to D\pi^0$, $D \to K_S^0\pi^+\pi^-$, $K_S^0 \to \pi^+\pi^-$, $\pi^0 \to \gamma\gamma$, $\eta \to \gamma\gamma$, $\pi^0\pi^+\pi^-$, $\eta' \to \eta\,\pi^+\pi^-$, and $\omega \to \pi^0\pi^+\pi^-$.

Charged tracks are considered to be pions. The K_S^0 candidate is reconstructed from $\pi^+\pi^-$ pairs, whose χ^2 probability of forming a common vertex is greater than 0.1%, with invariant mass within $10\,{\rm MeV}/c^2$ of the nominal K_S^0 mass [11]. The distance between the K_S^0 decay vertex and the primary interaction point projected on the x-y plane (perpendicular to the beam axis) is required to be greater than three times its measurement uncertainty. The angle θ_K between the K_S^0 momentum and the line connecting the production and decay vertices of the K_S^0 on the x-y plane is required to satisfy $\cos\theta_K > 0.992$.

An energy cluster in the electromagnetic calorimeter, isolated from any charged tracks and with the expected lateral shower shape for photons, is considered a photon candidate. A pair of photons forms a $\pi^0 \to \gamma\gamma$ ($\eta \to \gamma\gamma$) candidate if both photon energies exceed 30 (100) MeV and the invariant mass of the pair is between 100 and $160\,{\rm MeV}/c^2$ (508 and $588\,{\rm MeV}/c^2$). If the η is paired with a D^*, the invariant mass window is tightened to $515 < m_{\gamma\gamma} < 581\,{\rm MeV}/c^2$. The $\eta \to \gamma\gamma$ candidate is rejected if either photon, when combined with any other photon in the event, has an invariant mass within $6\,{\rm MeV}/c^2$ of the nominal π^0 mass. We perform a kinematic fit to the photon pair with its invariant mass constrained at the nominal π^0 or η mass and reject candidates with a fit probability less than 0.1%.

The $\eta/\omega \to \pi^0\pi^+\pi^-$, $\eta' \to \eta\,\pi^+\pi^-$, and $D \to K_S^0\pi^+\pi^-$ candidates are formed by combining a π^0, η, or K_S^0 with two charged pions. The χ^2 probability of the decay products coming from a common vertex for h^0 (D) is required to be greater than 0.1% (1%). The momentum of the π^0 and the η candidates used in ω and η' reconstruction must be greater than $200\,{\rm MeV}/c$. The invariant masses of the η, η', and ω candidates are required to be within 10, 8 and $18\,{\rm MeV}/c^2$ of their respective nominal masses, which correspond to approximately twice the RMS of the signal distributions. We retain D candidates within $60\,{\rm MeV}/c^2$ of the nominal D^0 mass, approximately 10 times its mass resolution, to include sufficient data in the sideband. A kinematic fit is performed on the D candidate to constrain its mass to the nominal

D^0 mass. A $D^* \to D\pi^0$ candidate is accepted if the invariant mass difference between D^* and D candidates is within $3\,\mathrm{MeV}/c^2$ of the nominal mass difference.

The signal is characterized by the kinematic variables $m_{\rm ES} \equiv \sqrt{(s/2 + \mathbf{p}_0 \cdot \mathbf{p}_B)^2/E_0^2 - \mathbf{p}_B^2}$, and $\Delta E \equiv E_B^* - E_{\rm beam}^*$, where the asterisk denotes the quantities evaluated in the center-of-mass (c.m.) frame, the subscripts 0, beam and B denote the e^+e^- system, the beam and the B candidate, respectively, and $\sqrt{s}$ is the c.m. energy. For signal events, $m_{\rm ES}$ peaks near the B^0 mass with a resolution of about $3\,\mathrm{MeV}/c^2$, and ΔE peaks near zero, with a resolution that varies by mode. We require $m_{\rm ES} > 5.23\,\mathrm{GeV}/c^2$ and select events with $|\Delta E| < 80\,\mathrm{MeV}$ for modes with $\pi^0, \eta \to \gamma\gamma$, and $|\Delta E| < 40\,\mathrm{MeV}$ for modes with $\eta, \omega \to \pi^0\pi^+\pi^-$, or $\eta' \to \eta\,\pi^+\pi^-$.

The proper decay time difference Δt is determined from the measured distance between the two B decay vertices projected onto the boost axis and the boost ($\beta\gamma = 0.56$) of the c.m. system. The reconstructed $|\Delta t|$ and its uncertainty $\sigma_{\Delta t}$ are required to satisfy $|\Delta t| < 15$ ps and $\sigma_{\Delta t} < 2.5$ ps. The flavor of $B_{\rm tag}$ is identified from particles that do not belong to the reconstructed B meson using a neural network based flavor-tagging algorithm [12].

The main background is from the continuum $e^+e^- \to q\overline{q}$ ($q = u, d, s, c$). We use a Fisher discriminant ($\mathcal{F}$) to separate the more isotropic $B\overline{B}$ events from more jet-like $q\overline{q}$ events [13]. The requirement on $\mathcal{F}$ is optimized with simulation. Another major background for the $D^*\pi^0$ mode comes from color-allowed $B^- \to D^0\rho^-(\rho^- \to \pi^0\pi^-)$ decays, which mimic signal if the π^- is missed from reconstruction while a random π^0 is included. We veto the B^0 candidate if the combination of another charged pion in the event with the D and the π^0 in the B^0 candidate is consistent with a charged B decay. In total we select 4450 events, of which 2843 events have useful tagging information (tagged).

The signal and background yields are determined by a fit to the $(m_{\rm ES}, m_D)$ distributions using a two-dimensional probability density function (PDF), where m_D denotes the $K^0_S\pi^+\pi^-$ invariant mass. We divide the sample into four categories to take into account different background levels: (1) $D\pi^0$, (2) $D\eta$ and $D\eta'$ (3) $D\omega$, and (4) D^*h^0. The PDF has five components: (a) signal, and backgrounds that peak in (b) both $m_{\rm ES}$ and m_D, (c) $m_{\rm ES}$ but not m_D, (d) m_D but not $m_{\rm ES}$, and (e) neither distribution. Both peaks are modeled by a Crystal Ball line shape [14]. The non-peaking component is modeled by a straight line in m_D and a threshold function [15] in $m_{\rm ES}$. We fit the four categories of events simultaneously, allowing the $m_{\rm ES}$ peak shape to be different but letting them share the m_D shape and $m_{\rm ES}$ background parameters. We first determine the amount of the peaking component (b) from simulated events and then fit to data allowing all other components to vary. We obtain 463 ± 39 signal events (335 ± 32 tagged). The contribution from each mode is shown in Table I. The $m_{\rm ES}$ and m_D distributions are shown in Fig. 1.

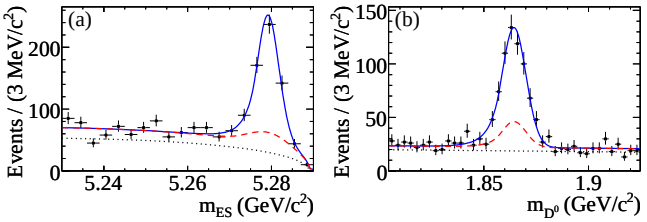

FIG. 1: Distributions of (a) $m_{\rm ES}$ [$|m_D - m_{D^0}^{\rm PDG}| < 14\,\mathrm{MeV}/c^2$], and (b) D mass [$m_{\rm ES} > 5.27\,\mathrm{GeV}/c^2$]. Dashed (dotted) lines represent the total (non-peaking) background.

The $D^0 \to K^0_S\pi^+\pi^-$ Dalitz plot has been studied in detail [16, 17]. We use the isobar formalism described in [18] to express $\mathcal{A}_{D^0}$ as a sum of two-body decay matrix elements ($\mathcal{A}_r$) and a non-resonant (NR) contribution,

$$\mathcal{A}_{D^0} = a_{\rm NR} e^{i\phi_{\rm NR}} + \sum_r a_r e^{i\phi_r} \mathcal{A}_r(m_+^2, m_-^2)\,. \qquad (3)$$

The function $\mathcal{A}_r(m_+^2, m_-^2)$ is the Lorentz-invariant expression for the matrix element of a D^0 decaying into $K^0_S\pi^+\pi^-$ through an intermediate resonance r, parameterized as a function of the position on the Dalitz plot. The resonances in the model include $K^*(892)$, $K_0^*(1430)$, $K_2^*(1430)$, $K^*(1410)$ and $K^*(1680)$ for both $K^0_S\pi^+$ and $K^0_S\pi^-$, and $\rho(770)$, $\omega(782)$, $f_0(980)$, $f_0(1370)$, $f_2(1270)$, $\rho(1450)$, and two scalar terms σ and σ' in the $\pi^+\pi^-$ system. Details of the Dalitz model and the parameters (determined from data) can be found in [17].

To perform the time-dependent Dalitz plot analysis, we expand the PDF to include Δt and Dalitz plot dependence. The signal component is proportional to expression 1, modified to account for the probability of mis-identifying the $B_{\rm tag}$ flavor (mistag), and is convolved with a sum of three Gaussian distributions [19]. The mistag parameters and the resolution function are determined from a large data control sample of $B^0 \to D^{(*)-}h^+$ decays, where h^+ is a π^+, ρ^+, or a_1^+ meson. Each of the background components consists of a product of Δt and (m_+^2, m_-^2) PDFs. The components that peak in m_D use $\mathcal{A}_{D^0}(m_+^2, m_-^2)$ as their Dalitz model. The model for components that are flat in m_D is an incoherent sum of a phase space contribution and several resonances. The choice of resonances and their relative contributions are determined empirically from events outside the m_D peak. The Δt model for components that peak in $m_{\rm ES}$ is a simple exponential decay convolved with the resolution function used in the signal component. For the non-peaking background, we use a zero-lifetime component convolved with a double-Gaussian resolution function for events with a real D because they are dominated by $c\overline{c}$ events, and we add an exponential decay component for events without a real D to account for B background.

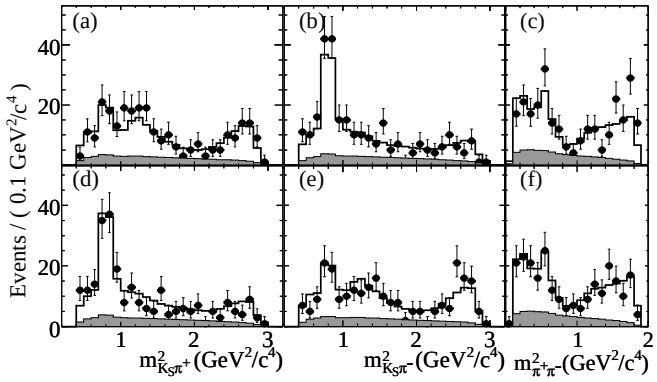

FIG. 2: Dalitz plot projections for (a,b,c) B^0-tagged events and (d,e,f) $\overline{B}^0$-tagged events. Points are data, open histograms are PDF projections, and shaded histograms are background contributions.

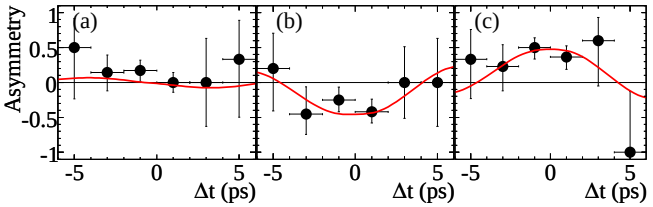

FIG. 3: Time-dependent asymmetries for (a) $D \to K^0_S\rho$ region ($|m_{\pi^+\pi^-} - 770| < 150$), where the opposite CP asymmetry in D^*h^0 has been taken into account, (b) $D \to K^{*+}\pi^-$ region, and (c) $D \to K^{*-}\pi^+$ region ($|m_{K^0_S\pi} - 892| < 50$). Units are MeV/$c^2$. Curves are projections of the PDF.

We fit the $m_{\rm ES}$, m_D, and Δt distributions, with $m_{\rm ES}$ and m_D shapes and background fractions fixed by the previous fit for event yields, to determine the Δt parameters for backgrounds. We then perform the final fit adding Dalitz plot variables to determine $\cos 2\beta$, $\sin 2\beta$ and $|\lambda|$. Table I shows the nominal fit result (All) and the results of a fit allowing $\cos 2\beta$ and $\sin 2\beta$ to be different among the four types of events. The correlations are $\rho(\cos 2\beta, \sin 2\beta) = 2\%$, $\rho(|\lambda|, \cos 2\beta) = 2\%$, and $\rho(|\lambda|, \sin 2\beta) = -2\%$. The Dalitz plot projections are shown in Fig. 2. Figure 3 shows the time-dependent asymmetries $(N_+ - N_-)/(N_+ + N_-)$, where $N_+(N_-)$ is the number of $B^0(\overline{B}^0)$ tagged events, for events in various Dalitz plot regions. Events in the $D \to K^0_S\rho$ region are dominated by a single CP eigenstate, thus the asymmetry is proportional to $\sin 2\beta \sin(\Delta m \Delta t)$. Events near $D \to K^{*\pm}\pi^{\mp}$ are dominated by decays to a definite flavor, and therefore exhibit a $\cos(\Delta m \Delta t)$ behavior.

TABLE I: Tagged event yields $N_{\rm tag}$ and fit results. Errors are statistical.

Mode	$N_{\rm tag}$	$\cos 2\beta$	$\sin 2\beta$	$\lvert\lambda\rvert$
$D\pi^0$	143 ± 19	0.78 ± 0.92	0.70 ± 0.52	1.0 (fixed)
$D\eta/\eta'$	60 ± 12	1.20 ± 1.19	-1.17 ± 1.00	
$D\omega$	76 ± 12	0.43 ± 0.87	-0.48 ± 0.74	
D^*h^0	56 ± 12	-0.56 ± 1.07	0.78 ± 0.87	
All	335 ± 32	0.42 ± 0.49	0.29 ± 0.34	1.01 ± 0.08

The dominant systematic uncertainty is the Dalitz plot model dependence. The Dalitz model includes scalar terms σ and σ', which are not well established, in order to achieve a good quality fit [17]. We study the effect of these two scalars by simulating a number of datasets, each of which is 50 times the size of the data, according to the PDF, and repeat the final fit using both the nominal PDF and the PDF without the two scalars. We compare the results between the two fits in each dataset and conservatively take the quadratic sum of the mean and RMS of the differences as the systematic uncertainty: $\sigma(\cos 2\beta) = 0.13$, $\sigma(\sin 2\beta) = 0.05$, and $\sigma(|\lambda|) < 0.01$. Many parameters are pre-determined in fits to control samples and to data without the Dalitz variables. We randomize them according to a Gaussian distribution whose width equals one standard deviation of each parameter, taking correlations into account, and repeat the final fit. The width of the distribution is taken as the systematic uncertainty: $\sigma(\cos 2\beta) = 0.06$, $\sigma(\sin 2\beta) = 0.02$ from Dalitz model parameters; $\sigma(\cos 2\beta) = 0.05$, $\sigma(\sin 2\beta) = 0.02$ from m_D and $m_{\rm ES}$ shape parameters; $\sigma(\cos 2\beta) \lesssim 0.01$, $\sigma(\sin 2\beta) \lesssim 0.01$ from background Δt parameters, tagging parameters, or signal Δt resolution function. We also vary the peaking background fractions by the statistical uncertainty found in simulation and find the variations are $\sigma(\cos 2\beta) = 0.02$ and $\sigma(\sin 2\beta) = 0.01$. Other sources of uncertainty such as B^0-$\overline{B}^0$ mixing frequency, B lifetimes, background Dalitz model and reconstruction efficiency variation over the Dalitz plot are negligible. In all cases, the uncertainty on $|\lambda|$ is less than 0.01. The only significant uncertainty on $|\lambda|$ (~ 0.02) is from the interference between the CKM-suppressed $\overline{b} \to \overline{u}c\overline{d}$ and CKM-favored $b \to c\overline{u}d$ amplitudes in some $B_{\rm tag}$ final states [20]. This effect is studied with simulation. Summing over all contributions in quadrature, we obtain total experimental systematic uncertainties $\sigma(\cos 2\beta) = 0.09$, $\sigma(\sin 2\beta) = 0.03$, and $\sigma(|\lambda|) = 0.02$.

To resolve the ambiguity in 2β, we generate two sets of toy simulation samples, one with $\cos 2\beta = \sqrt{1 - S_0^2} \equiv C_0$, and the other with $\cos 2\beta = -C_0$, where $S_0 = 0.678$, the world average of $\sin 2\beta$ [21], and fit each sample while fixing $\sin 2\beta = S_0$ and $|\lambda| = 1$. For data, this configuration results in $\cos 2\beta = 0.43 \pm 0.47$. We then use double-Gaussian functions, $h_\pm(x)$ for $\pm C_0$ hypotheses, to model the probability density of the resulting $\cos 2\beta$ distributions, smeared by the experimental systematic uncertainty and the uncertainty of C_0. The confidence level (C.L.) of preferring $\cos 2\beta = +C_0$ over $-C_0$ is defined as $h_+(x)/[h_+(x) + h_-(x)]$ if $\cos 2\beta = x$ is observed

in data. Considering the Dalitz model dependence for $\cos 2\beta$ (0.13), we use x between 0.43 ± 0.13 and find the smallest C.L.= 86% at $x = 0.43 - 0.13$.

In conclusion, we have studied the $B^0 \to D^{(*)}h^0$ decays using a time-dependent Dalitz plot analysis of $D \to K^0_S\pi^+\pi^-$. We obtain $\cos 2\beta = 0.42 \pm 0.49(\text{stat.}) \pm 0.09(\text{syst.}) \pm 0.13(\text{Dalitz})$, $\sin 2\beta = 0.29 \pm 0.34(\text{stat.}) \pm 0.03(\text{syst.}) \pm 0.05(\text{Dalitz})$, and $|\lambda| = 1.01 \pm 0.08(\text{stat.}) \pm 0.02(\text{syst.})$. Using the world average $\sin 2\beta = 0.678 \pm 0.026$ and $|\lambda| = 1$, $\cos 2\beta > 0$ is preferred over $\cos 2\beta < 0$ at 86% C.L.

We are grateful for the excellent luminosity and machine conditions provided by our PEP-II colleagues, and for the substantial dedicated effort from the computing organizations that support *BABAR*. The collaborating institutions wish to thank SLAC for its support and kind hospitality. This work is supported by DOE and NSF (USA), NSERC (Canada), CEA and CNRS-IN2P3 (France), BMBF and DFG (Germany), INFN (Italy), FOM (The Netherlands), NFR (Norway), MIST (Russia), MEC (Spain), and STFC (United Kingdom). Individuals have received support from the Marie Curie EIF (European Union) and the A. P. Sloan Foundation.

* Deceased
† Now at Tel Aviv University, Tel Aviv, 69978, Israel
‡ Also with Università di Perugia, Dipartimento di Fisica, Perugia, Italy
§ Also with Università della Basilicata, Potenza, Italy
¶ Also with Universitat de Barcelona, Facultat de Fisica, Departament ECM, E-08028 Barcelona, Spain

[1] B. Aubert *et al.* (*BABAR* Collaboration), Phys. Rev. Lett. **94**, 161803 (2005); K.-F. Chen *et al.* (Belle Collaboration), Phys. Rev. Lett. **98**, 031802 (2007).
[2] N. Cabibbo, Phys. Rev. Lett. **10**, 531 (1963); M. Kobayashi and T. Maskawa, Prog. Theoret. Phys. **49**, 652 (1973).
[3] B. Aubert *et al.* (*BABAR* Collaboration), Phys. Rev. D **71**, 032005 (2005); R. Itoh, Y. Onuki *et al.* (Belle Collaboration), Phys. Rev. Lett. **95**, 091601 (2005).
[4] P. Krokovny *et al.* (Belle Collaboration), Phys. Rev. Lett. **97**, 081801 (2006).
[5] B. Aubert *et al.* (*BABAR* Collaboration), Phys. Rev. D **74**, 091101 (2006); J. Dalseno *et al.* (Belle Collaboration), arXiv:0706.2045[hep-ex].
[6] B. Aubert *et al.* (*BABAR* Collaboration), submitted to Phys. Rev. Lett. (arXiv:0706.3885[hep-ex]).
[7] The notation $D^{(*)}$ represents $D^{(*)0}$ or $\overline{D}^{(*)0}$, or their linear combination.
[8] A. Bondar, T. Gershon and P. Krokovny, Phys. Lett. B **624**, 1 (2005).
[9] A. Bondar and T. Gershon, Phys. Rev. D **70**, 091503 (2004).
[10] B. Aubert *et al.* (*BABAR* Collaboration), Nucl. Instrum. Meth. A **479**, 1 (2002).
[11] All nominal masses are from W.-M. Yao *et al.* (Particle Data Group), J. Phys. G **33**, 1 (2006).
[12] B. Aubert *et al.* (*BABAR* Collaboration), Phys. Rev. Lett. **94**, 161803 (2005).
[13] B. Aubert *et al.* (*BABAR* Collaboration), submitted to Phys. Rev. Lett. [hep-ex/0703019].
[14] M.J. Oreglia, Ph.D Thesis, Stanford University [Report No. SLAC-236, 1980)], Appendix D; J.E. Gaiser, Ph.D Thesis, Stanford University [Report No. SLAC-255, 1982], Appendix F; T. Skwarnicki, Ph.D Thesis, Institute for Nuclear Physics, Krakow, [Report No. DESY F31-86-02, 1986], Appendix E.
[15] H. Albrecht *et al.* (ARGUS Collaboration), Phys. Lett. B **241**, 278 (1990).
[16] A. Poluektov *et al.* (Belle Collaboration), Phys. Rev. D **70**, 072003 (2004); A. Poluektov *et al.* (Belle Collaboration), Phys. Rev. D **73**, 112009 (2006).
[17] B. Aubert *et al.* (*BABAR* Collaboration), Phys. Rev. Lett. **95**, 121802 (2005).
[18] S. Kopp *et al.* (CLEO Collaboration), Phys. Rev. D **63**, 092001 (2001); H. Muramatsu *et al.* (CLEO Collaboration), Phys. Rev. Lett. **89**, 251802 (2002); Erratum-ibid: **90**, 059901 (2003).
[19] B. Aubert *et al.*(*BABAR* Collaboration), Phys. Rev. D **66**, 032003 (2002).
[20] O. Long *et al.*, Phys. Rev. D **68**, 034010 (2003).
[21] E. Barberio *et al.* (HFAG), arXiv:0704.3575[hep-ex], and online update at http://www.slac.stanford.edu/xorg/hfag